ARMY RESEARCH LABORATORY

Radiometric Measurements of Powerline Cables at 94 GHz

David A. Wikner and Thomas J. Pizzillo

ARL-TR-837

February 2001

Approved for public release; distribution unlimited.

20010314 043

The findings in this report are not to be construed as an official Department of the Army position unless so designated by other authorized documents.

Citation of manufacturer's or trade names does not constitute an official endorsement or approval of the use thereof.

Destroy this report when it is no longer needed. Do not return it to the originator.

Army Research Laboratory

Adelphi, MD 20783-1197

ARL-TR-837 **February 2001**

Radiometric Measurements of Powerline Cables at 94 GHz

David A. Wikner and Thomas J. Pizzillo

Sensors and Electron Devices Directorate

Approved for public release; distribution unlimited.

Abstract

When pilots are flying at low altitudes, they need a sensor that can help them detect and avoid wires; this need remains a high priority for all U.S. military services. Many different sensors have been considered to fulfill this need. This report presents data that were collected on powerline wires of various diameters with the use of a 94-GHz radiometer. These measurements were conducted at short range in an effort to quantify the wire signatures and to determine if a millimeter-wave radiometer could be used to help pilots avoid wires. Data are presented for seven sizes of wire as well as for the horizon background of each wire. The results show that wires down to 1/4 in. in diameter can probably be detected reliably at ranges up to 200 m with a 94-GHz radiometer that uses a 3-ft antenna, provided that the signature of the horizon background can be characterized during flight. Beyond 200 m, the results show that an image-enhancement algorithm, if proven to be adequate, or a larger antenna will probably be necessary to reliably detect most standard powerline wires.

Contents

1. Introduction 1

2. Experiment Description 2

3. Measurement Results/Discussion 4

4. Comparison With a Cylinder Model 7

5. Conclusions 10

References 11

Distribution 13

Report Documentation Page 15

Figures

1. Block diagram of ARL 94-GHz radiometer 2
2. Measurement scene from point of view of radiometer 3
3. Image of 11/16-in.-diam wire taken with ARL 94-GHz radiometer at a range of 4 m 4
4. Left graph shows vertical profile of brightness temperature for both 11/16-in. wire and background versus zenith angle 4
5. Left graph shows vertical profile of brightness temperature for both 1/2-in. wire and background versus zenith angle 4
6. Brightness temperature of background scene versus zenith angle for various background data runs 6
7. A calculation of expected wire contrast versus range 9

Tables

1. Physical characteristics of all wires measured during experiment 3
2. Summary of all data collected and results of cylinder calculation ... 6

1. Introduction

The U.S. military is greatly interested in finding a sensor that can help pilots detect and avoid wires when flying at low altitudes. The U.S. Army is particularly interested in preventing wire collisions with its helicopters, which often fly at an altitude of 200 ft or less during missions. The required sensor should operate effectively in the daytime, nighttime, and under reduced-visibility conditions. The type of sensor that ultimately will be used to fill this need is currently undetermined. Millimeter-wave (MMW) radar, ladar, and passive MMW imagers are all being considered [1–4]. We made the measurements presented in this report to assess the potential of an MMW radiometer to detect powerline wires by empirically determining the limits of the technology. From this information, we can weigh the benefits of radiometry against its limitations in a meaningful way.

An ARL 94-GHz radiometer was used to measure the signature of a variety of wire types and sizes at short range. In this report, we present these results and extrapolate them with range and antenna size to show results for many cases of interest. In addition, we have made theoretical calculations of the passive MMW signature of a bare metal cylinder for comparison.

2. Experiment Description

The experiment reported here measured the 94-GHz radiometric signature of a variety of powerline wires of known size at a known range. We accomplished this with the use of the Army Research Laboratory's 94-GHz Dicke-switched radiometer [5]. This instrument is used to measure the low-level, thermal MMW radiation emitted and reflected naturally by its environment. The voltage data collected are converted to a noise-equivalent temperature or brightness temperature by calibration software. Figure 1 shows a circuit diagram of the radiometer. The radiometer's noise figure of about 8 dB, instantaneous bandwidth of 6 GHz, and typical signal-integration time of 30 ms result in a system sensitivity of 0.2 K. For this experiment, the radiometer received vertically polarized radiation and was fitted with a 3-in.-diam horn-fed lens antenna that results in a 3-dB beamwidth of 2.75°. The switch in front of the mixer (as shown in the figure) is a ferrite device that operates over the bandwidth 91 to 97 GHz with a loss of 0.6 dB. It was switched at a rate of about 1 kHz during data collection to remove offset drift in the receiver circuit. The radiometer was calibrated before each measurement with the use of liquid-nitrogen-soaked radar-absorbing material. The radiometer is housed in a temperature-controlled box that is heated to 95 °F to minimize gain drifts between calibrations. This results in an absolute accuracy of about ±1 K for the system.

Wires of various diameters and materials were collected, and the signature of each one was carefully measured with the radiometer at short range so that the results could be extrapolated to longer range. Table 1 shows the wires that were measured. Each wire was about 2 m in length and was mounted in a fixture that held it horizontally in front of the radiometer at a range of about 4 m (fig. 2). This meant that the radiometer 3-dB far-field beam spot on each wire was approximately 6.2 in. (15.7 cm). In addition, each piece of wire was rotated relative to the radiometer such that the angle between the axis of the wire and the radiometer line of sight was about 45°.

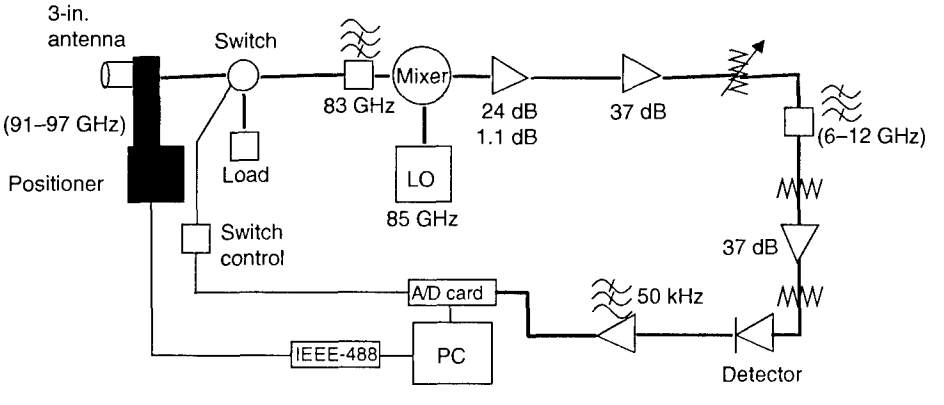

Figure 1. Block diagram of ARL 94-GHz radiometer.

Table 1. Physical characteristics of all wires measured during experiment.

Wire diameter (in.)	Strand diameter (in.)	Period of spiral (in.)	Description
1/4	1/16	3 3/8	Steel
5/16	1/8	4 15/16	1 center steel wire 7 Al outer wires
1/2	5/32	6	Al
11/16	1/8	8 15/16	1 copper center wire 18 Al outer wires
13/16	3/32	9 7/8	37-strand Al
15/16	1/16	N/A	5/32 cross-linked polystyrene outer layer
17/16	1/8	11 1/2	37-strand Al wire

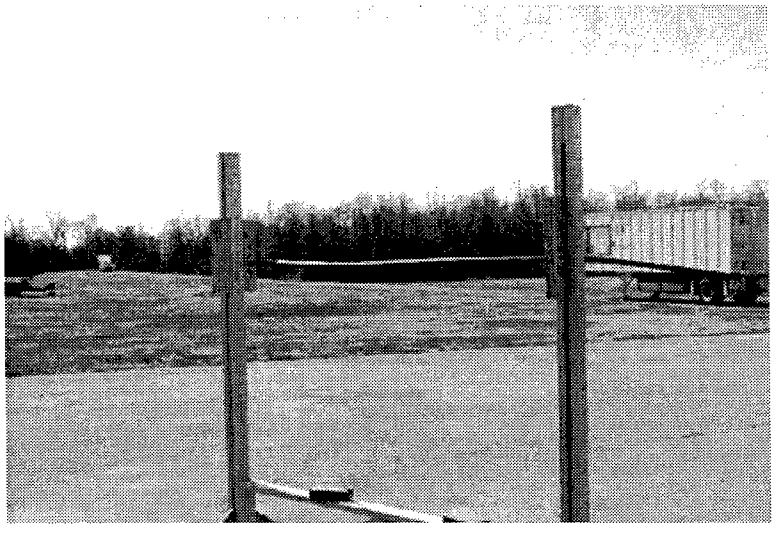

Figure 2. Measurement scene from point of view of radiometer. Shown is 15/16-in.-diam wire mounted in fixture.

This was done to minimize the reflections off the wire emitted by the building behind the radiometer; these reflections would have increased the measured brightness temperature of the wire. The 15/16-in. wire was clad in polystyrene (as indicated in the table). All other wires were bare metal.

We collected data on each wire by raster scanning the scene and forming an image of the wire and its background. The data were collected in half-beamwidth steps across the scene. A raster-scanned image of just the background with the wire removed was taken after each wire measurement to allow a comparison of the two images and to create background statistics. In addition, the zenith sky brightness temperature was measured after each wire measurement so that its effect on the scene could be quantified.

3. Measurement Results/Discussion

As stated in the previous section, we collected the data of each wire by raster scanning the radiometer's antenna beam over the scene. Figure 3 shows an example of such an image. The data were processed by extracting the portion of each image between the vertical wooden beams that supported the wire. This was done so that the beams did not enter into the data statistics. From this portion of the image, we averaged each horizontal line of data to a single value. This process results in a one-dimensional array that corresponds to an averaged vertical brightness-temperature profile of the image. We performed the process on each wire image and also for each background image taken without the wire present. Given a vertical profile for both the wire and its background, one can make a subtraction and plot the difference. Figures 4 and 5 show examples of data for two different wires that have been processed in this manner.

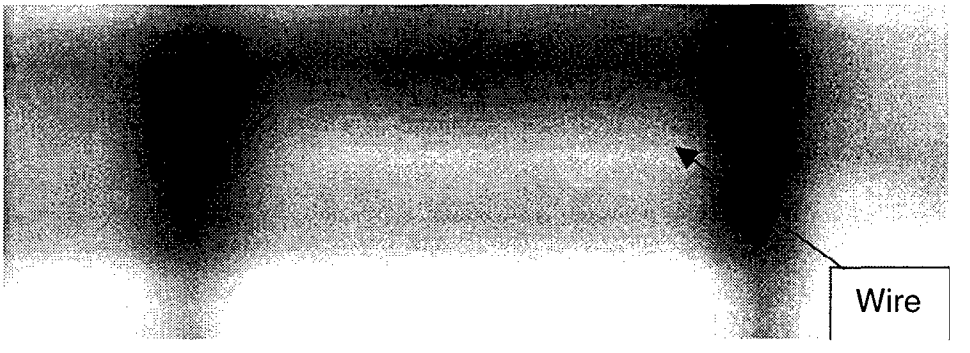

Figure 3. Image of 11/16-in.-diam wire taken with ARL 94-GHz radiometer at a range of 4 m. Dark vertical structures are due to vertical wooden pieces of fixture. Wire can be seen as a thin white line across middle of scene.

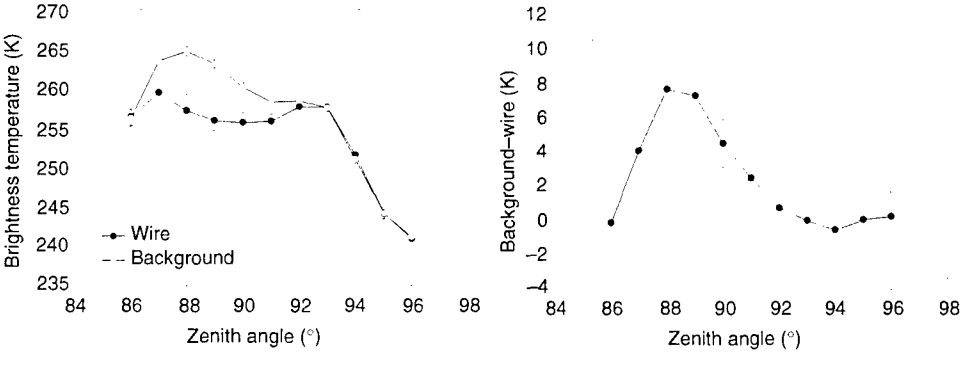

Figure 4. Left graph shows vertical profile of brightness temperature for both 11/16-in. wire and background versus zenith angle. Right graph shows difference between two plots.

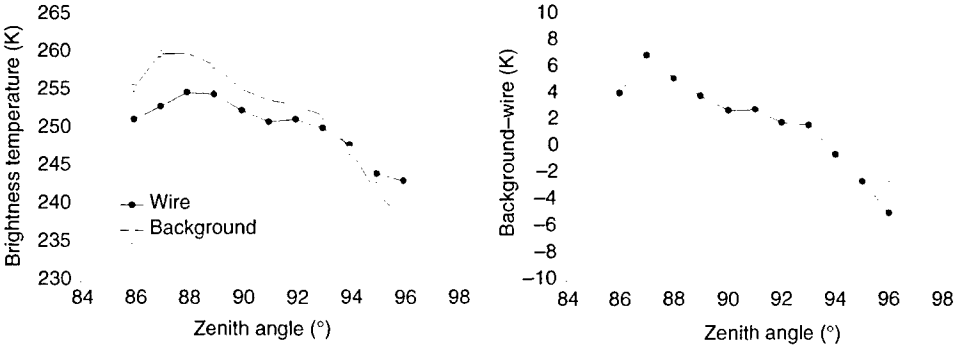

Figure 5. Left graph shows vertical profile of brightness temperature for both 1/2-in. wire and background versus zenith angle. Right graph shows difference between two plots.

The left-hand graph of each figure shows the vertical profile of the brightness temperature of each scene versus the angle from zenith. These graphs have two plots; one is the profile with the wire present and the other is the profile without the wire. The wire was located at a zenith angle around 88° and is seen in the figures to have a lower brightness temperature than the background. This is more apparent in the difference graph on the right-hand side of each figure. The background plots show that as the zenith angle increases above 93° (3° below the horizon), the standard deviations become larger. This is mostly because the radiometer is pointed at asphalt at these angles. A relatively large variability in brightness temperature that is often seen in asphalt is due to changes in solar loading and wind speed. On days that the data were taken, it was variably cloudy and cold; therefore, the physical temperature of the asphalt was not stable. Table 2 presents a summary of all wire data as well as sky-temperature data. The wire data shown are the maximum value of the difference between the background and the wire. The last two columns of the table show calculated model results that will be described later.

The differences seen in the table from wire to wire are due to a combination of a changing fill factor (the fractional area of the 3-dB spot occupied by the wire), variations in the background, and a changing sky temperature. The changing fill factor is obviously due to the varying wire size. The changing background brightness temperature is due mostly to variations in its physical temperature. Despite all these variables, one can see some trends in the data. The 1/2- and 11/16-in. wires show more contrast than the smaller wires, as expected, but the 13/16-, 15/16-, and 17/16-in. wires do not. The smaller than expected contrast for the 15/16-in. wire is likely due to attenuation caused by the outer polystyrene insulation around the cable. Additionally, it is likely that the 13/16- and 17/16-in. cables have a smaller than expected contrast because of an increased sky temperature. What is more significant, though, is that the contrast magnitudes are fairly small overall, especially when compared to the amount by which the background changes versus angle. If one studies all the background profiles taken during the test (fig. 6), one can clearly see that the variation is quite large compared to the signature of the wires. What is important to note, though, is that the shape of the curves is very similar near the horizon. (The shape below the horizon varies more as was discussed earlier.) Therefore, to detect wires, it may be necessary to collect a running brightness temperature template of the horizon during flight and look for changes in its shape to pull the small wire signal out from the horizon clutter.

Table 2. Summary of all data collected and results of cylinder calculation.

Wire diameter inches (m)	Zenith sky temperature (K)	Background brightness temperature (K)	Measured brightness temperature (background-wire) (K)	Weighted sky temperature (K)	Calculated brightness temperature (background-cylinder) (K)
1/4 (0.00635)	48	262	4.3	111	3.0
5/16 (0.00793)	33	262	4.5	100	4.0
1/2 (0.01270)	56	260	7.0	115	5.7
11/16 (0.01746)	42	266	7.5	108	8.6
13/16 (0.02064)	79	265	6.4	133	8.5
15/16 (0.02381)	39	264	5.5	105	—
17/16 (0.02699)	89	257	4.3	138	10.0

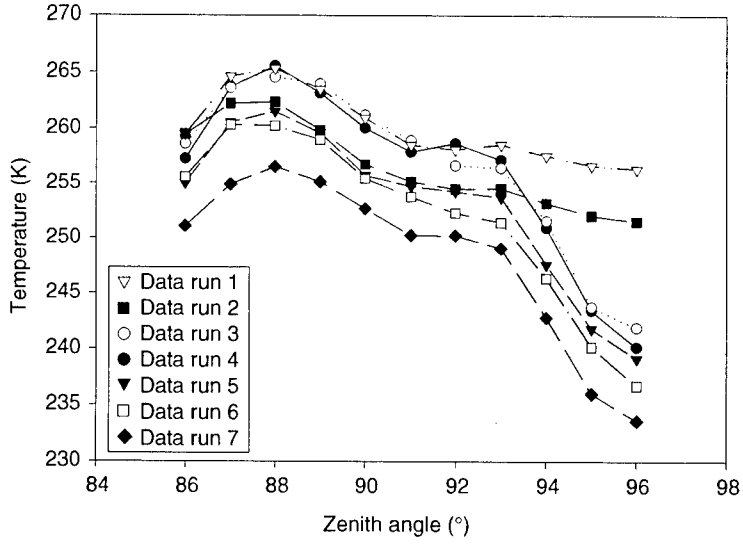

Figure 6. Brightness temperature of background scene versus zenith angle for various background data runs.

4. Comparison With a Cylinder Model

A simple model can be used to estimate the expected brightness temperature of metal cylinders of sizes that match those of the measured wires. Imagine a perfectly reflecting metal cylinder that is much longer than the radiometer's antenna beam spot is wide and that runs across the middle of the beam spot. If the diameter of the circular beam spot is much larger than the diameter of the cylinder, then the shape of the wire can be considered rectangular and the fraction of the spot filled by the cylinder (fill factor) can be expressed as a ratio of the areas

$$f = \frac{\Theta R d}{\pi\left(\frac{\Theta R}{2}\right)^2} = \frac{4d}{\pi\Theta R}. \tag{1}$$

In this expression, f is the fill factor, d is the diameter of the cylinder, Θ is the radiometer 3-dB beamwidth in radians, and R is the range from the radiometer to the cylinder. If the radiometer is about the same height above the ground as the cylinder, then the top half of the cylinder will reflect MMW energy from the sky and the bottom half will reflect MMW energy from the ground (assuming other objects are not nearby, e.g., trees, buildings). Therefore, the contrast between a pixel that contains the cylinder and a pixel without the cylinder can be expressed

$$\Delta T = b - \left(\frac{f}{2} * s + \left(1 - \frac{f}{2}\right) b\right), \tag{2}$$

where b is the background-brightness temperature without a wire present and s is the sky temperature. The fill factor, f, has been divided by two because only half the cylinder reflects energy from the sky. The sky-brightness temperature increases as a cosine function from the zenith-brightness temperature to the horizon-brightness temperature. Therefore, the s used in this equation is a cosine-weighted average of those two values, since the cylinder reflects all sky angles toward the radiometer. Table 2 shows these values. Inserting equation (1) into equation (2) gives

$$\Delta T = (b - s)\frac{2d}{\pi\Theta R}. \tag{3}$$

Equation (3) shows the expected $1/R$ dependence of the contrast and a linear dependence on wire diameter that is valid for $d << \Theta R$. Note that signal path attenuation has been ignored, since it is negligible at the ranges involved.

Table 2 shows the calculated ΔTs for the cylinders along with the measured data for the same-sized wire. We made each calculation for a particular cylinder size, sky-brightness temperature, and background-brightness temperature, and the values we used are shown in the table. We made the

calculations with the use of the same range and antenna size as the measurements. Several points can be made about the calculated data. One is that the brightness temperature differences do not go up linearly with wire diameter, as equation (3) would seem to imply since b and s were not constant. This is simply because the sky and background temperature values used in the model were varied with cylinder size according to the measured values (e.g., the 1/2-in. cylinder calculation uses the 1/2-in. wire sky-brightness temperature data). The 11/16- and 13/16-in. cylinders show about the same signature despite their size difference because a warmer sky temperature was used for the 13/16-in. cylinder calculation as shown in the table. The 15/16-in. wire had an attenuating outer layer of polystyrene that was not modeled, so no calculated results are given for it. In general, though, the model results trend upward with increasing cylinder size as expected.

A comparison of the model with the calculated values, however, shows significant differences. The measured wire data show no meaningful trends with wire size, which can be explained by one difficulty with the measurement technique. As figure 6 shows, the background brightness temperature can vary appreciably between the time the scene is measured with the wire and the time the scene is measured without it. If nothing changed during that period of time, then the corresponding background and wire curves should lie on top of one another except at angles where the wire is present. Clearly this is not always the case. Figure 4 shows a good correspondence between the wire and background data, but figure 5 does not. In effect, this changing background adds about 5 K of noise to the ΔT measurement. This means that because of the way the data were collected, they are not sensitive enough to determine the effect of diameter on the MMW brightness temperature of a wire. The data do show, however, the order of magnitude of the signal that can be expected under the test parameters given here. This conclusion is supported by the fact that the cylinder calculations are close to the measured data.

Given the magnitude of the brightness-temperature differences shown by table 2 and the fact that the data were taken at a 4-m range with a 3-in. antenna, we can extrapolate the data to longer ranges and larger antennas. These data provide a rough measure of what is possible with this type of sensor at ranges of interest. Based on the data in this report, figure 7 shows the temperature differences that would be expected versus range for a radiometer with a 3-ft-diam antenna. After recalculating the fill factor, we see that the measured values have simply been extrapolated out in range. The curves follow the expected $1/R$ dependence evident in equation (3). The graph shows that, under the environmental conditions of the measurement, the brightness-temperature change caused by a wire is on the order of 1 K between 200 and 400 m. A radiometer would require a sensitivity of about 0.2 K to detect this change, which is realistic for a W-band radiometer that has a 30-ms integration time.

Figure 7. A calculation of expected wire contrast versus range. Curves are a calculated extrapolation based on data collected for each wire. Radiometer antenna diameter was taken to be 3 ft.

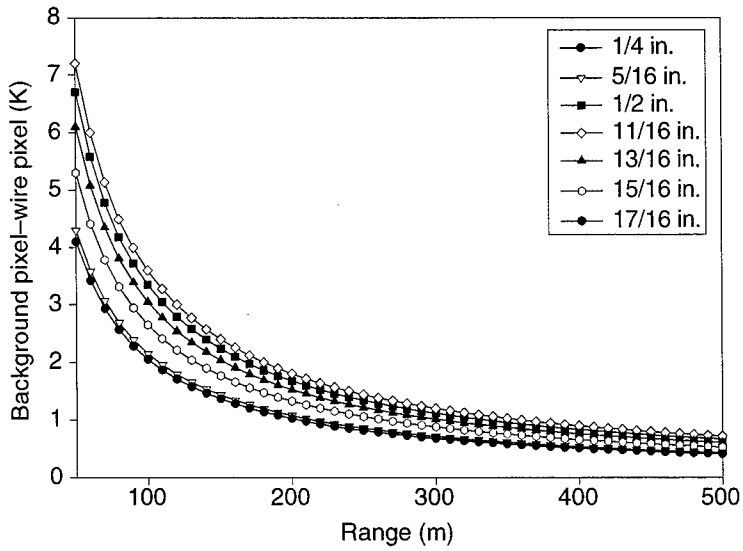

A significant challenge in the use of an MMW radiometer to detect wires is clearly the variation and fluctuation of the background. The data show that the background temperature changes by ±4 K at angles, near the horizon. This problem is complicated by the fact that an airborne radiometer may be viewing the horizon scene from a variety of angles, depending on its orientation. The simplest way to solve this problem may be to have the sensor continuously take data of the horizon during flight and store an averaged template to which each new piece of data could be compared. Testing this idea would require either sophisticated modeling of this scenario or flight testing.

Before this effort is undertaken, however, one should thoroughly address the issue of varying weather. The data in this report show qualitatively the effect of a changing sky-brightness temperature on the wire-brightness temperature. Larger wires sometimes showed lower than expected contrast because of a higher sky-brightness temperature. Overall, though, the sky temperatures measured during this test were fairly low. It is not unusual to have zenith sky temperatures of 125 to 175 K on humid summer days. This would tend to reduce wire contrast. On the other hand, a humid summer day would raise the background-brightness temperature and therefore tend to increase wire contrast. The seasonal effects on contrast should certainly be considered more thoroughly to assess the range of contrasts that might be encountered.

It should also be noted that no sophisticated image processing has been applied to the data. Some algorithms such as maximum entropy and 2-mu have demonstrated an ability to enhance contrast for some types of objects in an image. Future work could involve trying these or similar algorithms to determine if a contrast improvement can be made that might extend the usable range of a radiometric sensor.

5. Conclusions

We have presented the results of 94-GHz radiometric measurements of powerline wires. We collected data on wires of a variety of diameters and compared them to the background of each wire. The background data showed a large variation in brightness temperature around the horizon, but measurable differences were detected when a wire was present in the scene. We made calculations to determine the MMW brightness temperature of cylinders under the same conditions as those of the wire experiment. The results showed that such a method comes close to predicting the magnitude of the actual wire data. We extrapolated the wire data to a longer range scenario simulating a radiometer with a 3-ft antenna. The extrapolated data show that wire-to-background contrast is marginally sufficient for detection out to ranges of 400 m. The use of an 8-dB signal-to-noise ratio criterion shows that reliable detection would occur out to about 200 m. We can conclude that individual wires down to 1/4 in. in diameter can probably be detected reliably at ranges less than 200 m with a 94-GHz radiometer that uses a 3-ft antenna, with the condition that the MMW emission of the horizon background can be characterized during flight. Beyond 200 m, the results show that an image-enhancement algorithm or a larger diameter antenna will probably be necessary to reliably detect most standard powerline wires. The possibility exists, however, that groups of wires could be detected reliably at greater ranges (>400 m) because of the increased pixel-fill factor. Since wires are usually found in groups of two, three, or more, this scenario should be considered in future measurements. Additional measurements with the use of polarimetry could also be considered to explore possible improvements in wire-to-clutter ratio.

References

1. N. A. Salmon, "*W*-band real-time passive millimeter-wave imager for helicopter collision avoidance," *Aerosense 99*, Proc. SPIE **3703** (April 1999), pp 28–32.
2. P. Cerchie, B. Shipley, R. Aust, J. Wasson, and D. Reago, "Manned simulation results concerning design parameters for an effective obstacle avoidance system (OASYS)," *J. Am. Helicopter Society* **37**, No. 2 (April 1992), pp 3–10.
3. R. J. Grasso, A. C. Pratty, C. M. Vann, C. G. Stimson, and J. E. Ackleson, "OASYS laser radar characterization of natural and manmade terrestrial features," Proc. SPIE **3870** (April 1999), pp 620–631.
4. L. D. Almsted, R. C. Becker, and R. E. Zelenka, "Affordable MMW aircraft collision avoidance system," Proc. SPIE **3088** (April 1997), pp 57–63.
5. D. Wikner and T. Pizzillo, "Measurement of nadir and near-nadir 94-GHz brightness temperatures of several tactical scene clutter materials," *Aerosense 99*, Proc. SPIE **3703** (7 April 1999), pp 102–113.

Distribution

Admnstr
Defns Techl Info Ctr
ATTN DTIC-OCP
8725 John J Kingman Rd Ste 0944
FT Belvoir VA 22060-6218

DARPA
ATTN MTO R Balcerak
ATTN TTO LTC COL B Tousley
3701 N Fairfax Dr
Arlington VA 22203-1714

Under Secy of Defns for Rsrch & Engrg
ATTN Rsrch & Advncd Techlgy
Depart of Defns
Washington DC 20310

Dpty Assist Secy for Rsrch & Techlgy
ATTN SARD-TT M Andrews
The Pentagon
Washington DC 20310-0103

NVESD
ATTN AMSEL-RD-NV J Ratches
ATTN AMSEL-RD-NV-ASD D Reago
ATTN AMSEL-RD-NV-TISD F Petito
ATTN Techl Lib
10221 Burbeck Rd Ste 430
FT Belvoir VA 22060-5806

US Army AMCOM/AATD
ATTN AMSAM-AR-T-I B Buckanin
Bldg 401
FT Eustis VA 23604-5577

US Army Armament RDEC
ATTN SMCAR-FSP-A1 M Rosenbluth
Picatinny Arsenal NJ 07806-5000

US Army Avn & Mis Cmnd
ATTN AMSAM-RD-MG-RF G Emmons
Redstone Arsenal AL 35898-5253

US Army CRREL
ATTN G D Ashton
72 Lyme Rd
Hanover NH 03755-1290

US Army Materiel Sys Anal Actvty
ATTN AMXSY-MP
Aberdeen Proving Ground MD 21005

US Army Mis Lab
ATTN AMSAM-RD-AS-RPR Redstone Sci Info Ctr
ATTN AMSAM-RD-AS-RPT Techl Info Div
ATTN AMSAM-RD Advanced Sensors Dir
ATTN AMSAM-RD Sys Simulation & Dev Dir
Redstone Arsenal AL 35809

US Army Test & Eval Cmnd
ATTN STEWS-TE-AF F Moreno
ATTN STEWS-TE-LG S Dickerson
White Sands Missile Range NM 88002

USATEC
ATTN J N Rinker
7701 Telegraph Rd
Alexandria VA 22315-3864

Nav Rsrch Lab
ATTN 4555 W Waters
ATTN 7223 G Poe
ATTN 7223 S Highley
4555 Overlook Ave SW
Washington DC 20375

Nav Surfc Weapons Ctr
ATTN DX-21 Library Div
Dahlgren VA 22448

Nav Weapons Ctr
ATTN 38 Rsrch Dept
ATTN 381 Physics Div
China Lake CA 93555

USAF Wright Lab
ATTN WL/MMGS R Smith
101 W Eglin Blvd Ste 287A
Eglin AFB FL 32542-6810

Sandia Natl Lab
PO Box 5800
Albuquerque NM 87185

Distribution (cont'd)

NASA Goddard Spc Flight Ctr
ATTN D M Le Vine
ATTN J Wang
ATTN P Racette
Greenbelt MD 20771

Georgia Inst of Techlgy
Georgia Tech Rsrch Inst
ATTN Radar & Instrmntn Lab T L Lane
Atlanta GA 30332

Univ of Massachusetts at Amherst
College of Engrg
ATTN C Swift
Amherst MA 01003

Trex Enterprises Corp
ATTN J Galliano
ATTN J Lovberg
10455 Pacific Center Court
San Diego CA 92121

TRW Spc & Techlgy Div
ATTN M Shoucri
ATTN P Moffa
One Space Park
Redondo Beach CA 90278

Veridian/ERIM
ATTN IRIA Lib
PO Box 134001
Ann Arbor MI 48113-4001

NASA Langley Rsrch Ctr
ATTN B Kendall
Mail Stop 490
Hampton VA 23681-0001

US Army Rsrch Lab
ATTN AMSRL-SE-RM R Bender
ATTN AMSRL-SE-RM R Tan
ATTN AMSRL-SE-RM S Stratton
ATTN AMSRL-WM-BA R A McGee
Aberdeen Proving Ground MD 21005

Director
US Army Rsrch Lab
ATTN AMSRL-RO-D JCI Chang
ATTN AMSRL-RO-EL J Harvey
PO Box 12211
Research Triangle Park NC 27709-2211

US ARDEC
ATTN AMSRL-SE-RM S Weiss
Adelphi MD 20783-1197

US Army Rsrch Lab
ATTN AMSRL-D D R Smith
ATTN AMSRL-DD J M Miller
ATTN AMSRL-CI-AI-R Mail & Records Mgmt
ATTN AMSRL-CI-AP Techl Pub (2 copies)
ATTN AMSRL-CI-LL Techl Lib (2 copies)
ATTN AMSRL-SE J Pellegrino
ATTN AMSRL-SE-EE Z G Sztankay
ATTN AMSRL-SE-R A Sindoris
ATTN AMSRL-SE-R B Wallace
ATTN AMSRL-SE-RM C Ly
ATTN AMSRL-SE-RM D Hutchins
ATTN AMSRL-SE-RM D W Vance
ATTN AMSRL-SE-RM D Wikner (10 copies)
ATTN AMSRL-SE-RM E Adler
ATTN AMSRL-SE-RM E Burke
ATTN AMSRL-SE-RM G Goldman
ATTN AMSRL-SE-RM H Dropkin
ATTN AMSRL-SE-RM J Clark
ATTN AMSRL-SE-RM J Nemarich
ATTN AMSRL-SE-RM J Silverstein
ATTN AMSRL-SE-RM J Silvious
ATTN AMSRL-SE-RM J Speulstra
ATTN AMSRL-SE-RM K Tom
ATTN AMSRL-SE-RM R Dahlstrom
ATTN AMSRL-SE-RM R Harris
ATTN AMSRL-SE-RM R Wellman
ATTN AMSRL-SE-RM T Pizzillo (10 copies)
ATTN AMSRL-SE-RM W Wiebach
ATTN AMSRL-SE-SE T Kipp
Adelphi MD 20783-1197

REPORT DOCUMENTATION PAGE

Form Approved
OMB No. 0704-0188

Public reporting burden for this collection of information is estimated to average 1 hour per response, including the time for reviewing instructions, searching existing data sources, gathering and maintaining the data needed, and completing and reviewing the collection of information. Send comments regarding this burden estimate or any other aspect of this collection of information, including suggestions for reducing this burden, to Washington Headquarters Services, Directorate for Information Operations and Reports, 1215 Jefferson Davis Highway, Suite 1204, Arlington, VA 22202-4302, and to the Office of Management and Budget, Paperwork Reduction Project (0704-0188), Washington, DC 20503.

1. AGENCY USE ONLY *(Leave blank)*	2. REPORT DATE	3. REPORT TYPE AND DATES COVERED
	February 2001	Final, 1 Jan to 31 Jan 2000

4. TITLE AND SUBTITLE Radiometric Measurements of Powerline Cables at 94 GHz

5. FUNDING NUMBERS
DA PR: A142
PE: 62120A

6. AUTHOR(S) David A. Wikner and Thomas J. Pizzillo

7. PERFORMING ORGANIZATION NAME(S) AND ADDRESS(ES)
U.S. Army Research Laboratory
Attn: AMSRL-SE-RM email: wikner@arl.army.mil
2800 Powder Mill Road
Adelphi, MD 20783-1197

8. PERFORMING ORGANIZATION REPORT NUMBER
ARL-TR-837

9. SPONSORING/MONITORING AGENCY NAME(S) AND ADDRESS(ES)
U.S. Army Research Laboratory
2800 Powder Mill Road
Adelphi, MD 20783-1197

10. SPONSORING/MONITORING AGENCY REPORT NUMBER

11. SUPPLEMENTARY NOTES
ARL PR: 0NEMHH
AMS code: 622120.142

12a. DISTRIBUTION/AVAILABILITY STATEMENT Approved for public release; distribution unlimited.

12b. DISTRIBUTION CODE

13. ABSTRACT *(Maximum 200 words)*

When pilots are flying at low altitudes, they need a sensor that can help them detect and avoid wires; this need remains a high priority for all U.S. military services. Many different sensors have been considered to fulfill this need. This report presents data that were collected on powerline wires of various diameters with the use of a 94-GHz radiometer. These measurements were conducted at short range in an effort to quantify the wire signatures and to determine if a millimeter-wave radiometer could be used to help pilots avoid wires. Data are presented for seven sizes of wire as well as for the horizon background of each wire. The results show that wires down to 1/4 in. in diameter can probably be detected reliably at ranges up to 200 m with a 94-GHz radiometer that uses a 3-ft antenna, provided that the signature of the horizon background can be characterized during flight. Beyond 200 m, the results show that an image-enhancement algorithm, if proven to be adequate, or a larger antenna will probably be necessary to reliably detect most standard powerline wires.

14. SUBJECT TERMS Radiometry, millimeter-wave, collision avoidance, powerline cables

15. NUMBER OF PAGES 19

16. PRICE CODE

17. SECURITY CLASSIFICATION OF REPORT	18. SECURITY CLASSIFICATION OF THIS PAGE	19. SECURITY CLASSIFICATION OF ABSTRACT	20. LIMITATION OF ABSTRACT
Unclassified	Unclassified	Unclassified	UL

NSN 7540-01-280-5500

Standard Form 298 (Rev. 2-89)
Prescribed by ANSI Std. Z39-18
298-102